

# Multifunctional Cholinesterase and Amyloid Beta Fibrillization Modulators. Synthesis and Biological Investigation

Stefania Butini,<sup>†,‡</sup> Margherita Brindisi,<sup>†,‡</sup> Simone Brogi,<sup>†,‡</sup> Samuele Maramai,<sup>†,‡</sup> Egeria Guarino,<sup>†,‡</sup> Alessandro Panico,<sup>†,‡</sup> Ashima Saxena,<sup>§</sup> Ved Chauhan,<sup>||</sup> Raffaella Colombo,<sup>⊥</sup> Laura Verga,<sup>#</sup> Ersilia De Lorenzi,<sup>⊥</sup> Manuela Bartolini,<sup>▽</sup> Vincenza Andrisano,<sup>○</sup> Ettore Novellino,<sup>†,¶</sup> Giuseppe Campiani,<sup>\*,†,‡</sup> and Sandra Gemma<sup>†,‡</sup>

<sup>†</sup>European Research Centre for Drug Discovery and Development—NatSynDrugs and <sup>‡</sup>Dipartimento di Biotecnologie, Chimica e Farmacia, University of Siena, via Aldo Moro 2, 53100 Siena, Italy

<sup>§</sup>Division of Biochemistry, Walter Reed Army Institute of Research, Silver Spring, Maryland 20910, United States

<sup>||</sup>Institute for Basic Research in Developmental Disabilities, Forest Hill Road, Staten Island, New York 10314, United States

<sup>⊥</sup>Dipartimento di Scienze del Farmaco, University of Pavia, viale Taramelli 12, 27100 Pavia, Italy

<sup>▽</sup>Department of Pathology, Fondazione IRCCS, Policlinico S. Matteo and University of Pavia, 27100 Pavia, Italy

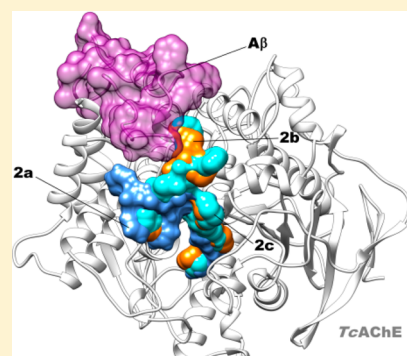
<sup>○</sup>Department of Pharmacy and Biotechnology, University of Bologna, via Belmeloro 6, 40126 Bologna, Italy

<sup>#</sup>Department for Life Quality Studies, University of Bologna, Corso di Augusto 237, 47900 Rimini, Italy

<sup>¶</sup>Dipartimento di Farmacia, University of Napoli Federico II, via D. Montesano 49, 80131 Napoli, Italy

## S Supporting Information

**ABSTRACT:** In order to identify novel Alzheimer's modifying pharmacological tools, we developed bis-tacrine bearing a peptide moiety for specific interference with surface sites of *human acetylcholinesterase* (*hAChE*) binding amyloid-beta (*A $\beta$* ). Accordingly, compounds **2a–c** proved to be inhibitors of *hAChE* catalytic and noncatalytic functions, binding the catalytic and peripheral sites, interfering with *A $\beta$*  aggregation and with the *A $\beta$*  self-oligomerization process (**2a**). Compounds **2a–c** in complex with *TcAChE* span the gorge with the bis-tacrine system, and the peptide moieties bulge outside the gorge in proximity of the peripheral site. These moieties are likely responsible for the observed reduction of *hAChE*-induced *A $\beta$*  aggregation since they physically hamper *A $\beta$*  binding to the enzyme surface. Moreover, **2a** was able to significantly interfere with *A $\beta$*  self-oligomerization, while **2b,c** showed improved inhibition of *hAChE*-induced *A $\beta$*  aggregation.



**KEYWORDS:** Cholinesterase inhibitors, amyloid beta-peptides, multifunctional tools, amyloid beta oligomers, Alzheimer's disease, bivalent ligands

Convergent biochemical and genetic evidence suggest that the formation of amyloid-beta peptides (*A $\beta$* ) deposits in the brain is an important seminal step in the development of Alzheimer's disease (AD). The assembly of *A $\beta$*  into a variety of oligomeric and fibrillar species is one of the causal factors of AD. *A $\beta$*  oligomers have been shown to accelerate neuron cell death and are therefore thought to precipitate synaptic dysfunction. The inhibition of *A $\beta$*  oligomerization could thus provide a novel approach for treating the underlying cause of AD.<sup>1</sup> This latter aspect could be combined to inhibition of cholinesterases (ChE) catalytic activity and to interference with acetylcholinesterase (AChE) accelerated *A $\beta$*  aggregation in a single disease-modifying anti-Alzheimer's drug (DMAAD). The multifactorial nature of AD indeed supports a therapeutic approach based on multitarget directed ligands.<sup>2</sup> Currently available therapies for AD are only symptomatic,<sup>3</sup> and inhibition of AChE and butyrylcholinesterase (BuChE) is to

date the most established therapeutic approach.<sup>4–6</sup> AChE interacts with *A $\beta$*  by a mechanism involving its peripheral anionic site (PAS), and it was proposed that AChE may accelerate the deposition of *A $\beta$*  into fibrils<sup>7</sup> (noncatalytic function of AChE).<sup>8–11</sup> Further studies indicate that BuChE also colocalizes with *A $\beta$*  in senile plaques, and may play a role in plaques maturation.<sup>12</sup> While deposition of *A $\beta$*  plaques is the hallmark of the disease, the neurotoxicity of *A $\beta$*  oligomers was shown to be stronger than that of the fibrils.<sup>13,14</sup> Therefore, innovative DMAAD should also possess inhibition properties against *A $\beta$*  self-association. On these bases, we have developed a new set of multifunctional pharmacological tools that inhibit *A $\beta$*  self-association and oligomerization, the enzymatic activity

Received: July 25, 2013

Accepted: October 6, 2013

Published: October 6, 2013



of ChEs, and (to a moderate extent) the AChE-induced  $\text{A}\beta$  aggregation (**2a–c**, Figure 1). Tacrine-based bisfunctional

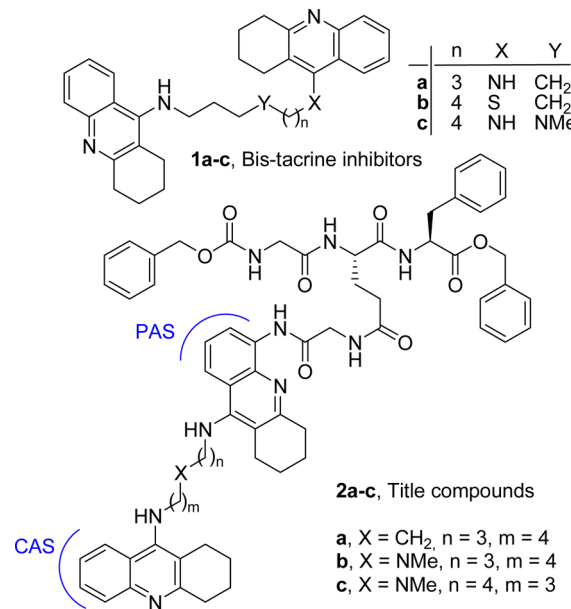


Figure 1. Reference and title compounds.

ligands inhibit AChE hydrolytic activity,<sup>15</sup> and in some cases, they interfere with its noncatalytic functions (binding to  $\text{A}\beta$ ), by interacting with AChE PAS (W279, *Torpedo californica* AChE (*TcAChE*) numbering).<sup>10,15–18</sup> Such inhibitors span the

active-site gorge, and the nature of the linker affects the affinity for AChE and BuChE (dual or triple sites inhibitors **1a–c**, Figure 1).<sup>15</sup> In order to develop innovative multifunctional pharmacological tools, based on our previous experience, we synthesized compounds **2a–c** (Figure 1) by combining a bis-tacrine scaffold (for achieving *h*ChEs inhibition) with a hydrophobic peptidomimetic sequence to interfere with the putative surface binding region of  $\text{A}\beta$  around W279, thus interfering with AChE-induced  $\text{A}\beta$  aggregation and  $\text{A}\beta$  self-association.<sup>13</sup>

Molecular modeling studies (Figure 2) and biological studies (Table 1 and Figure 3) confirmed our working hypothesis.

Table 1. Inhibition of *h*ChEs,  $\text{A}\beta_{1-42}$  Spontaneous, and *h*AChE-Induced  $\text{A}\beta_{1-40}$  Aggregation

compd	$K_i$ (nM) hAChE <sup>a</sup>	$K_i$ (nM) hBuChE <sup>a</sup>	hAChE/ hBuChE	$\text{A}\beta_{1-42}$ aggreg at 5 $\mu\text{M}$ (%) <sup>b</sup>	$\text{A}\beta_{1-40}$ hAChE- induced aggreg (%) <sup>b</sup>
<b>1a</b>				8.4 <sup>c</sup>	68 <sup>e</sup>
<b>1b</b>	28.0	1.65	16.9	NT	NT
<b>1c</b>	0.012	0.82	0.01	NT	50
<b>6</b>	0.78	0.06	13	NT	NT
<b>7</b>	0.23	8.26	0.028	NT	NT
<b>2a</b>	1.92	49.8	0.038	81	26
<b>2b</b>	5.02	61.77	0.081	NT	42
<b>2c</b>	1.48	21.26	0.070	51 <sup>d</sup>	42 <sup>f</sup>

<sup>a</sup>SD were within 10% of the mean. <sup>b</sup>SEM were within 10% of the mean. <sup>c</sup>Ref 19. <sup>d</sup> $\mu\text{M}$  IC<sub>50</sub> value (protocol 1, Supporting Information); <sup>e</sup>Ref 20. <sup>f</sup>IC<sub>50</sub> value = 113 ± 9  $\mu\text{M}$ ; NT stands for not tested.

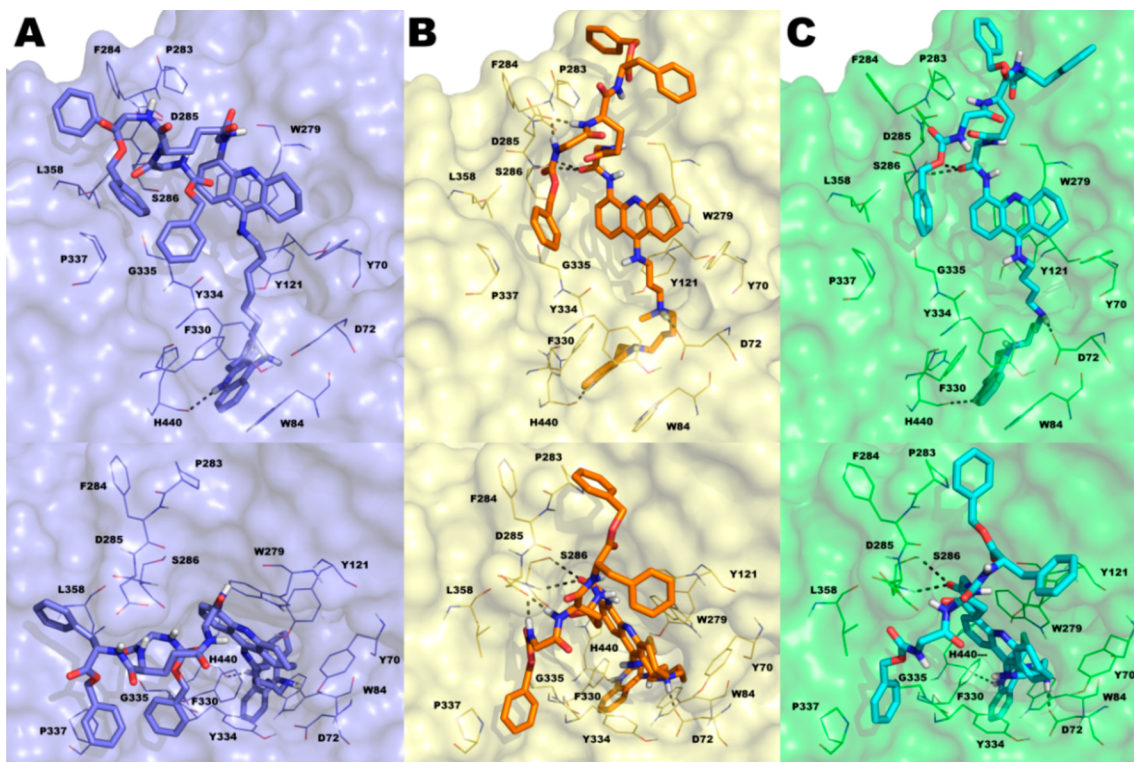
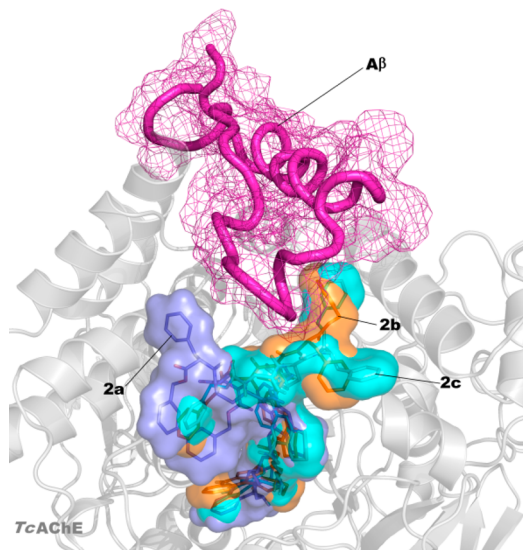


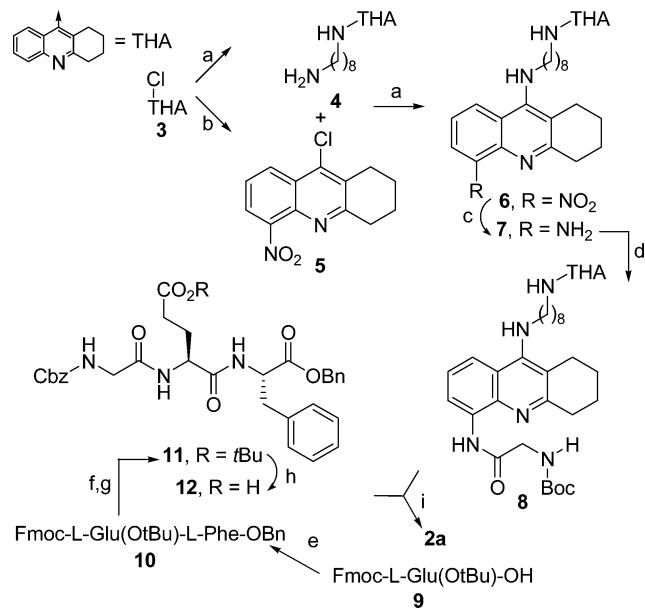
Figure 2. Docked poses of compounds **2a–c** into the *TcAChE* binding site (key residues are represented by lines) obtained using IFD protocol: (A) **2a** (blue sticks, blue surface for protein, glide XP score: -19.603 kcal/mol); (B) **2b** (orange sticks, yellow surface for protein, glide XP score: -20.561 kcal/mol); (C) **2c** (cyan sticks, green surface for protein, glide XP score: -21.143 kcal/mol). H-bonds were reported as gray dotted lines. Nonpolar hydrogens were omitted for clarity. The picture was generated by PyMOL.



**Figure 3.** Superposition of the docked pose of  $\text{A}\beta$  (magenta) in complex with  $\text{TcAChE}$  (HADDOCK web server version) with IFD poses of **2a** (blue), **2b** (orange), and **2c** (cyan) in complex with  $\text{TcAChE}$ .

Particularly, molecular docking procedure within  $\text{TcAChE}$  provided a clear-cut vision of the interaction pattern of **2a–c** with  $\text{TcAChE}$  catalytic site (CAS), PAS, and its surrounding surface area, allowing rationalization of the experimental data. The synthesis of compounds **2a–c** is reported in Scheme 1 of the Main Text and Scheme 1SI of the Supporting Information; discussion of the procedure is given in the Supporting

**Scheme 1. Synthesis of Compound **2a****<sup>a</sup>



<sup>a</sup>Reagents and conditions: (a)  $\text{K}_2\text{CO}_3$ , ( $\pm$ )-BINAP,  $\text{Pd}(\text{OAc})_2$ , and 1,8-diaminoctane (for **4**), 1,4-dioxane, reflux, 12 h, 62–65%; (b)  $\text{H}_2\text{SO}_4/\text{HNO}_3$ , from 0 °C to rt, 30', 50%; (c)  $\text{SnCl}_2 \cdot 2\text{H}_2\text{O}$ , EtOH, rt, 12 h, 60%; (d)  $\text{N-Boc-Gly-OH}$ , ethylchloroformate, THF-DCM, from -10 °C to rt, 3 h, 55%; (e) L-Phe-OBn, EDCI, HOEt, TEA, rt, 12 h, 93%; (f) DEA/DCM, rt, 1 h, 99%; (g) Z-Gly-OH, EDCI, HOEt, TEA, rt, 12 h, 65%; (h)  $\text{HCOOH}$ , rt, 3 h, 99%; (i) (1)  $\text{MeCOCl}$ ,  $\text{MeOH}$ , rt, 10', 99%; (2) **12**, EDCI, HOEt, TEA, from 0 °C to rt, 12 h, 42%.

Information. Biological data are reported in Table 1. The inhibition tests performed on  $\text{hChEs}$  revealed that **2a** (as well as precursors **6** and **7**) is a potent reversible inhibitor of  $\text{hChEs}$  ( $K_{ih\text{AChE}} = 1.9 \text{ nM}$ ,  $K_{ih\text{BuChE}} = 40.9 \text{ nM}$ ). Although both ChEs colocalize with  $\text{A}\beta$  plaques, **2a** was only tested against  $\text{hAChE}$ -induced  $\text{A}\beta_{1-40}$  aggregation. It also exhibited potent inhibition of  $\text{A}\beta_{1-42}$  spontaneous aggregation (81% at 5  $\mu\text{M}$ ). The potency of **2a** against  $\text{hAChE}$ -induced  $\text{A}\beta$  aggregation was improved using the tether of **1c**, one of the most potent inhibitors of  $\text{hAChE}$  known to date.<sup>15</sup> The selection was based on its specific interaction with the three identified recognition sites of the  $\text{hAChE}$  gorge (observed by docking studies using  $\text{hAChE}$ ),<sup>15</sup> which pushes the PAS oriented tacrine moiety to establish a triple  $\pi-\pi$  stacking with W286 and Y72 thus inducing a rotation of W286 ( $\text{hAChE}$  numbering).<sup>15</sup> Accordingly **2b,c** demonstrated higher ability to inhibit  $\text{hAChE}$   $\text{A}\beta$  aggregation while maintaining nM inhibition potency for  $\text{hChEs}$ .

These data were rationalized by means of molecular modeling studies performed on **1c** and **2a–c** in complex with  $\text{TcAChE}$ , which allowed us to directly compare results with those obtained from the crystal structure of **1b** in complex with  $\text{TcAChE}$  (PDB: 2CEK)<sup>16</sup> (X-ray studies of **2a** were performed on  $\text{TcAChE}$ <sup>21</sup>), even though the compounds were tested on human proteins.<sup>22</sup> We applied the Induced Fit Docking (IFD) protocol.<sup>23</sup> The IFD output for **1c** is shown in Figure 1SI, Supporting Information and those for **2a–c** are shown in Figures 2 and 2SI, Supporting Information. The reported docked solutions, belonging to the most populated clusters, show very high glide XP scores (higher than those obtained for the other clusters; Table 1SI, Supporting Information) thus representing the most reliable binding mode to  $\text{TcAChE}$ . By comparison of the X-ray complex of **1b** and dockings of **2a–c** with  $\text{TcAChE}$ , we observed that while the bis-tacrine moieties of **2a–c** spans the gorge as **1b** and other bis-tacrine inhibitors, the distal peptide-like moiety binds on the surface of the enzyme, in the vicinity of the PAS with different binding modes (Figure 2 A vs B, C). Furthermore, the terminal tacrine moiety of **2a–c** stacks in front of W279 (Figure 2). F330 undergoes a conformational change with the side chain rotated with respect to the native enzyme, in analogy to one alternate conformation of F330 in 2CEK. In contrast to 2CEK, where the W279 is rotated of 90°, our computational approach revealed that W279 nearly overlaps the native conformation when **2a–c** are bound (Figure 3SI, Supporting Information). The replacement of a methylene with an NMe in the linker between the tacrine moieties (**2b,c**) allows the formation of an additional polar interaction with the key midgorge residue D72 not observed in the complex with **2a** (Figure 2, top panels). Besides hydrophobic contacts with F330, Y70, Y121, and Y334, there is one H-bond between the protonated N of the CAS-interacting tacrine of **2a–c** and H440 (Figures 2 and 2SI, Supporting Information). Our computational analysis also indicated that the interactions with D72 may be responsible for the substantial differences observed in the disposition of the aromatic moieties of the peptide-like substructure of our compounds at the surface level. Particularly, for **2a** all the aromatic moieties project toward the same direction with the benzyl ester engaged in hydrophobic interactions with P337 and L358. Contrarily, for compounds **2b,c**, the same interactions are maintained by the benzylcarbamate moiety while the phenylalanine group and the benzyl ester moiety point toward an opposite direction (Figure 2, bottom panels).

It is worthy of note that these moieties, although solvent exposed, lay in close proximity to P283 and F284 (Figure 2 bottom panels B–C), which have already been identified as relevant for binding  $\text{A}\beta$ .<sup>8</sup> This evidence is in line with the higher experimentally determined potency of **2b,c** in inhibiting *hAChE* induced  $\text{A}\beta$  aggregation with respect to **2a**. As shown in Figure 3, the peptidic aromatic groups of **2b,c** may physically hamper  $\text{A}\beta$  binding to the surface of the enzyme. Moreover, the peptide-like structure of **2b,c** is maintained anchored to the surroundings of the PAS by H-bonds established between a carbonyl and two NH groups with S286 and D285, respectively, for **2b**, while for **2c** only H-bonds with S286 backbone and side chain were established by the Gly carbonyl group of the ligand (Figures 2 and 2SI, Supporting Information). For bisfunctional **1a** and **1c**, we confirmed that rotation of W279 at PAS may contribute to the inhibition potency of *hAChE*-induced  $\text{A}\beta$  aggregation since W279 is one of the residues critical for  $\text{A}\beta$  binding. In the case of peptide-based inhibitors **2a–c**, it becomes relevant the positioning of the aromatic moieties protruding outside the AChE gorge (e.g., **2c**,  $\text{IC}_{50} = 113 \mu\text{M}$ ) since W279 remains in the apoform position (Figure 3SI, Supporting Information).

Molecular modeling (Figures 2 and 3) and biological studies (Table 1) confirmed this hypothesis, being that **2b,c** is more potent than **2a** against *hAChE*-induced  $\text{A}\beta_{1-42}$  aggregation, while maintaining nM potency for *hChEs* inhibition. Furthermore, **2a,c** were tested for inhibition of  $\text{A}\beta_{1-42}$  spontaneous aggregation. Both compounds exhibited good inhibition properties (Table 1). These encouraging data prompted us to further explore the possible mechanism involved in these antifibrillogenic effects. We investigated the ability of **2a** to influence the  $\text{A}\beta_{1-42}$  oligomerization process. A capillary electrophoresis (CE) approach, associated with transmission electron microscopy (TEM) analysis,<sup>24,25</sup> demonstrated that **2a** induces a concentration-dependent interference with the oligomerization kinetics, preventing toxic oligomers and fibril formation. We confirmed that **2a** can perturb the formation kinetics of oligomeric intermediate species that were hypothesized to be the real effectors of the neurological damage. Figure 4A shows the control electropherograms after  $\text{A}\beta_{1-42}$  dissolution (see Supporting Information and Figure 4SI for details), where toxic oligomers increase over time (peak B area %  $77.2 \pm 0.9$  ( $t_0$ ,  $n = 3$ ) and  $91.4 \pm 1.6$ , (6 h,  $n = 3$ ) at the expenses of peak A, which is completely depleted on the fourth day from solubilization). Nonbranching  $\text{A}\beta$  fibrils were present in the precipitated sample (Figure 4D). With  $200 \mu\text{M}$  **2a**, a stabilization of oligomer growth occurs (peak B area %  $82.5 \pm 1.1$  ( $t_0$ ,  $n = 3$ ) and  $87.2 \pm 2.4$  (6 h,  $n = 3$ )), and on the second day, the oligomeric species were not detected (Figure 4B). Disaggregation of the toxic oligomers and precipitation are accelerated, if compared to  $\text{A}\beta_{1-42}$  alone, and amorphous aggregates are formed in place of fibrils (Figure 4E). Figure 4C shows a more potent and concentration-dependent activity (**2a**,  $500 \mu\text{M}$ ). Freshly solubilized  $\text{A}\beta_{1-42}$  does not form toxic, high molecular weight aggregates (peak B), while smaller oligomers (peak A) are detectable and stable only within 24 h (not shown). The TEM analysis (Figure 4F) shows amorphous aggregates. The addition of  $50 \mu\text{M}$  **2a** revealed amorphous aggregates at the TEM ( $n = 2$ , not shown). Thus, it seems that at higher **2a** concentrations ( $\text{A}\beta/\text{2a}$  ratio 1:2 and 1:5) a clear, concentration- and time-dependent depletion of higher molecular weight oligomers occurs (Figure 4B–C), which also produces fibrillogenesis inhibition (Figure 4E,F). Further,

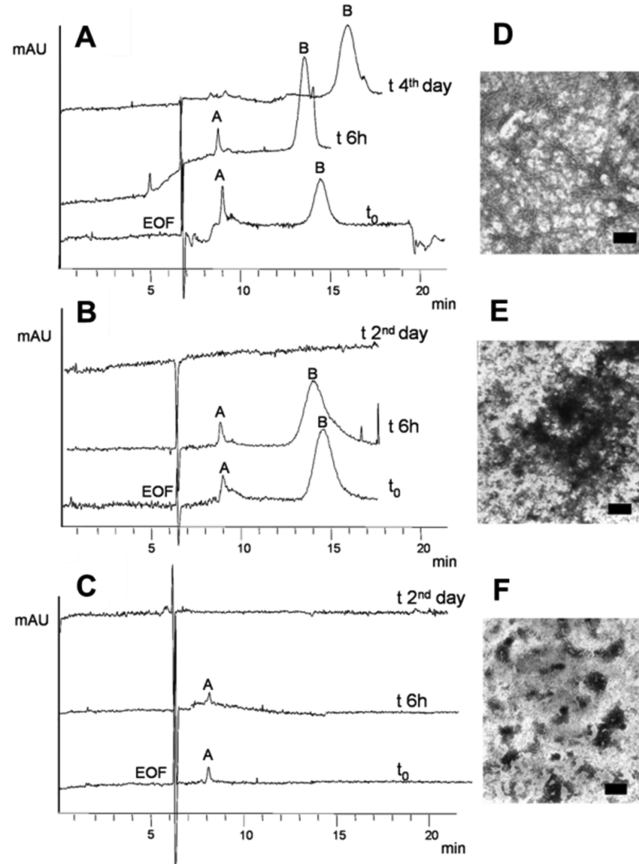


**Figure 4.** CE and TEM results: (A) control  $\text{A}\beta_{1-42}$  ( $100 \mu\text{M}$ ); (B)  $\text{A}\beta_{1-42}$  ( $100 \mu\text{M}$ ) incubated with **2a** ( $200 \mu\text{M}$ ); (C)  $\text{A}\beta_{1-42}$  ( $100 \mu\text{M}$ ) incubated with **2a** ( $500 \mu\text{M}$ ); (D–F) correspondent TEM images ( $n = 3$ ), scale bar = 100 nm.

**2a** ( $200$  and  $500 \mu\text{M}$ ) is able to disaggregate preformed fibrils, as from TEM analysis (not shown).

In conclusion, we describe the synthesis and biological characterization of novel multifunctional tools for the development of innovative DMAADs. Compound **2a** was able to interfere with  $\text{A}\beta$  self-oligomerization, while **2c** was found as a good inhibitor of *hAChE*-induced  $\text{A}\beta$  aggregation. Biological data demonstrate that binding the surface surrounding the PAS is not correlated to a high potency of inhibition of *hAChE*-induced  $\text{A}\beta$  aggregation (being **2a** a moderate inhibitor). On the contrary, introduction of a midgorge recognition site in the tether between the two tacrines (**2b,c**) pushes their peptide portion to occupy the surface where P283 and F284 are critical for  $\text{A}\beta$  binding. Compounds **2a–c** are prototypic of a new class of multifunctional ChEs inhibitors characterized by high potency for enzyme inhibition, for inhibition of *hAChE*-induced  $\text{A}\beta$  aggregation, and for inhibition of  $\text{A}\beta$  self-aggregation and oligomerization.

## ASSOCIATED CONTENT

### Supporting Information

Further CE notes, supplementary figures and table, details for synthesis, analytical data, and biological studies. This material is available free of charge via the Internet at <http://pubs.acs.org>.

## AUTHOR INFORMATION

### Corresponding Author

\*(G.C.) Tel: 0039 0577 234172. Fax: 0039 0577 234254. E-mail: campiani@unisi.it.

### Funding

We acknowledge NatSynDrugs, the Italian Ministry of University and Research (Project PRIN 2009Z8YTYC, and 2010M2JARJ\_008), Prog. Reg. Lombardia SAL-45 ID17261, and Unirimini S.p.A. for financial support.

### Notes

The authors declare no competing financial interest.

## ACKNOWLEDGMENTS

We acknowledge Prof. Marco Racchi for toxicity studies on oligomers. Opinions or assertions contained here are private views of the authors and are not to be construed as official or as reflecting true views of the Department of the Army or the Department of Defence.

## ABBREVIATIONS

$\text{A}\beta$ , Amyloid-beta peptides; AD, Alzheimer's disease; ChE, cholinesterase; AChE, acetylcholinesterase; DMAAD, disease-modifying anti-Alzheimer's drug; BuChE, butyrylcholinesterase; PAS, peripheral anionic site; CAS, catalytic site; TcAChE, *Torpedo californica* AChE; hAChE, human AChE; hBuChE, human BuChE; ( $\pm$ )-BINAP, ( $\pm$ )-2,2'-bis(diphenylphosphino)-1,1'-binaphthalene; THF, tetrahydrofuran; DCM, dichloromethane; EDCI, 1-ethyl-3-(3-dimethylaminopropyl)-carbodiimide; TEA, triethylamine; DEA, diethylamine; CE, capillary electrophoresis; TEM, transmission electron microscopy

## REFERENCES

- (1) Lauren, J.; Gimbel, D. A.; Nygaard, H. B.; Gilbert, J. W.; Strittmatter, S. M. Cellular prion protein mediates impairment of synaptic plasticity by amyloid-beta oligomers. *Nature* **2009**, *457*, 1128–1132.
- (2) Cavalli, A.; Bolognesi, M. L.; Capsoni, S.; Andrisano, V.; Bartolini, M.; Margotti, E.; Cattaneo, A.; Recanatini, M.; Melchiorre, C. A small molecule targeting the multifactorial nature of Alzheimer's disease. *Angew. Chem., Int. Ed.* **2007**, *46*, 3689–3692.
- (3) Sadowski, M.; Wisniewski, T. Disease modifying approaches for Alzheimer's pathology. *Curr. Pharm. Des.* **2007**, *13*, 1943–1954.
- (4) McShane, R.; Areosa Sastre, A.; Minakaran, N. Memantine for dementia. *Cochrane Database Syst. Rev.* **2006**, CD003154.
- (5) Cummings, J. L. Treatment of Alzheimer's disease: current and future therapeutic approaches. *Rev. Neurol. Dis.* **2004**, *1*, 60–69.
- (6) Greenblatt, H. M.; Dvir, H.; Silman, I.; Sussman, J. L. Acetylcholinesterase: a multifaceted target for structure-based drug design of anticholinesterase agents for the treatment of Alzheimer's disease. *J. Mol. Neurosci.* **2003**, *20*, 369–383.
- (7) Alvarez, A.; Opazo, C.; Alarcon, R.; Garrido, J.; Inestrosa, N. C. Acetylcholinesterase promotes the aggregation of amyloid-beta-peptide fragments by forming a complex with the growing fibrils. *J. Mol. Biol.* **1997**, *272*, 348–361.
- (8) De Ferrari, G. V.; Canales, M. A.; Shin, I.; Weiner, L. M.; Silman, I.; Inestrosa, N. C. A structural motif of acetylcholinesterase that promotes amyloid beta-peptide fibril formation. *Biochemistry* **2001**, *40*, 10447–10457.
- (9) Soreq, H.; Seidman, S. Acetylcholinesterase: new roles for an old actor. *Nat. Rev. Neurosci.* **2001**, *2*, 294–302.
- (10) Bartolini, M.; Bertucci, C.; Cavrini, V.; Andrisano, V. beta-Amyloid aggregation induced by human acetylcholinesterase: inhibition studies. *Biochem. Pharmacol.* **2003**, *65*, 407–416.
- (11) Reyes, A. E.; Chacon, M. A.; Dinamarca, M. C.; Cerpa, W.; Morgan, C.; Inestrosa, N. C. Acetylcholinesterase-Abeta complexes are more toxic than Abeta fibrils in rat hippocampus: effect on rat beta-amyloid aggregation, laminin expression, reactive astrocytosis, and neuronal cell loss. *Am. J. Pathol.* **2004**, *164*, 2163–2174.
- (12) Darvesh, S.; Cash, M. K.; Reid, G. A.; Martin, E.; Mitnitski, A.; Geula, C. Butyrylcholinesterase is associated with beta-amyloid plaques in the transgenic APPSWE/PSEN1dE9 mouse model of Alzheimer disease. *J. Neuropathol. Exp. Neurol.* **2012**, *71*, 2–14.
- (13) Benilova, I.; Karan, E.; De Strooper, B. The toxic Abeta oligomer and Alzheimer's disease: an emperor in need of clothes. *Nat. Neurosci.* **2012**, *15*, 349–357.
- (14) Hamley, I. W. The amyloid beta peptide: a chemist's perspective. Role in Alzheimer's and fibrillization. *Chem. Rev.* **2012**, *112*, 5147–5192.
- (15) Butini, S.; Campiani, G.; Borriello, M.; Gemma, S.; Panico, A.; Persico, M.; Catalaniotti, B.; Ros, S.; Brindisi, M.; Agnusdei, M.; Fiorini, I.; Nacci, V.; Novellino, E.; Belinskaya, T.; Saxena, A.; Fattorusso, C. Exploiting protein fluctuations at the active-site gorge of human cholinesterases: further optimization of the design strategy to develop extremely potent inhibitors. *J. Med. Chem.* **2008**, *51*, 3154–3170.
- (16) Colletier, J. P.; Sanson, B.; Nacher, F.; Gabellieri, E.; Fattorusso, C.; Campiani, G.; Weik, M. Conformational flexibility in the peripheral site of *Torpedo californica* acetylcholinesterase revealed by the complex structure with a bifunctional inhibitor. *J. Am. Chem. Soc.* **2006**, *128*, 4526–4527.
- (17) Pang, Y. P.; Quiram, P.; Jelacic, T.; Hong, F.; Brimijoin, S. Highly potent, selective, and low cost bis-tetrahydroaminoacrine inhibitors of acetylcholinesterase. Steps toward novel drugs for treating Alzheimer's disease. *J. Biol. Chem.* **1996**, *271*, 23646–23649.
- (18) Camps, P.; Formosa, X.; Galdeano, C.; Gomez, T.; Munoz-Torrero, D.; Ramirez, L.; Viayna, E.; Gomez, E.; Isambert, N.; Lavilla, R.; Badia, A.; Clos, M. V.; Bartolini, M.; Mancini, F.; Andrisano, V.; Bidon-Chanal, A.; Huertas, O.; Dafni, T.; Luque, F. J. Tacrine-based dual binding site acetylcholinesterase inhibitors as potential disease-modifying anti-Alzheimer drug candidates. *Chem. Biol. Interact.* **2010**, *187*, 411–415.
- (19) Minarini, A.; Milelli, A.; Tumiatti, V.; Rosini, M.; Simoni, E.; Bolognesi, M. L.; Andrisano, V.; Bartolini, M.; Motori, E.; Angeloni, C.; Hrelia, S. Cystamine-tacrine dimer: a new multi-target-directed ligand as potential therapeutic agent for Alzheimer's disease treatment. *Neuropharmacology* **2012**, *62*, 997–1003.
- (20) Bolognesi, M. L.; Cavalli, A.; Valgimigli, L.; Bartolini, M.; Rosini, M.; Andrisano, V.; Recanatini, M.; Melchiorre, C. Multi-target-directed drug design strategy: from a dual binding site acetylcholinesterase inhibitor to a trifunctional compound against Alzheimer's disease. *J. Med. Chem.* **2007**, *50*, 6446–6449.
- (21) Sanson, B. Dynamique structurale de l'acétylcholinestérase étudiée par cristallographie aux rayons X et par une méthode spectroscopique complémentaire. Ph.D. Thesis, Université Joseph Fourier, Grenoble I, 2009; see <http://www.ibs.fr/science/production-scientifique/theses-soutenues-a-l-ibs/?lang=fr>. The refined X-ray structure will be reported elsewhere.
- (22) Molecular modelling studies on hChEs will be reported elsewhere.
- (23) Schrödinger Suite 2011 Induced Fit Docking; Glide version 5.7; Prime version 3.0; Schrödinger, LLC: New York, 2011.
- (24) Sabella, S.; Quaglia, M.; Lanni, C.; Racchi, M.; Govoni, S.; Caccialanza, G.; Calligaro, A.; Bellotti, V.; De Lorenzi, E. Capillary electrophoresis studies on the aggregation process of beta-amyloid 1–42 and 1–40 peptides. *Electrophoresis* **2004**, *25*, 3186–3194.
- (25) Colombo, R.; Carotti, A.; Catto, M.; Racchi, M.; Lanni, C.; Verga, L.; Caccialanza, G.; De Lorenzi, E. CE can identify small molecules that selectively target soluble oligomers of amyloid beta protein and display antifibrillrogenic activity. *Electrophoresis* **2009**, *30*, 1418–1429.